The Mean Firing Rate of Atrial Fibrillation as Estimated from the ECG Evaluation Using a Biophysical Model

M Lemay[1], V Jacquemet[2], F Jousset[1], JM Vesin[1], A van Oosterom[3]

[1]Signal Processing Institute, Ecole Polytechnique Fédérale de Lausanne, Lausanne, Switzerland
[2]Department of Biomedical Engineering, Duke University, Durham, USA
[3]Division of Cardiology, Centre Hospitalier Universitaire Vaudois, Lausanne, Switzerland

Abstract

The correspondence between the firing rates of atrial myocytes during atrial fibrilation and the dominant frequencies observed in the Fourier spectra of the corresponding surface ECG signals was studied. The observations were based on signals simulated using a biophysical model of the atria and of the volume conduction effects of the thorax. Different substrates for AF were generated, each resulting in a different type of AF dynamics. The results indicate that the full Fourier spectrum yields more information on the complexity of a particular variant of AF than the analysis of just its dominant frequency. The same applies to analyzing the spectra of multiple leads rather using just single lead signals.

1. Introduction

The diagnosis of atrial fibrillation (AF) has been mainly based on visual inspection of the surface electrocardiogram (ECG), and limited to establishing its presence or absence [1]. The increasing incidence of this -most common- type of human cardiac arrhythmia has stimulated a wide range of research. During AF, instead of a single electrical activation wavefront traveling over the atria as under normal conditions, self-sustained multiple reentrant waves propagate in a chaotic manner over the atrial surface. On the ECG, instead of the normal P waves, continuous and apparently disorganized fibrillatory waves are observed.

The underlying mechanisms of the wavefront dynamics of AF relate to their substrates, which manifest themselves on different time scales. Invasive electrophysiological as well as non-invasive studies based on the surface ECG have used the dominant frequency (DF) for characterizing these time scales [2–4]. The DF is the modal frequency in the Fourier spectrum of the atrial signal, in invasive studies: the electrogram, in non-invasive studies: ECG lead signal. In the latter situation the DF is usually estimated on the signal of lead V1 after first suppressing the ECG components related to the ventricular activity [4, 5]. Lead V1 is the lead having its sensing electrode closest to the atria, the other lead signals are generally not considered.

In 2006, Jason Ng *et al* published the results of an invasive study [6] in which the firing rates of atrial myocytes and the DFs in atrial electrograms were compared. Their conclusion was that the time course of the DFs correlate well with that of the firing rate.

In our study the correspondence between firing rate of the atrial myocytes and the Fourier spectrum of ECG lead signals DFs is analyzed on the basis of signals numerically simulated by using a biophysical model of the human atria embedded in a realistic inhomogeneous model of the volume conduction aspects within the thorax. Various different substrates were created. The results pertaining to two specific variants are presented, selected from the two ends of the range of AF complexity, respectively.

2. Methods

2.1. Simulated atrial signals

A previously developed biophysical model of the atria was used to simulate the propagation of the electrical impulse in a realistic, thick-walled 3D model of atrial geometry [7]. Inside, propagation was simulated using a reaction-diffusion system (monodomain formulation) based on a detailed ionic model of the cell membrane kinetics proposed by Courtemanche *et al* [8, 9]. The numerical implementation of the method comprised a total of 800,000 coupled units.

To create a substrate for AF, different sets of modifications in the normal membrane parameters of the units were introduced aimed at reducing action potential duration and/or propagation velocity [9]. AF was induced by cross-shock or rapid pacing protocols, applied at different locations. Of the different realizations of sustained AF cre-

ated in this manner, two cases are presented. For Case I the membrane properties were changed uniformly, and resulted in a slow propagation. For Case II patched inhomogeneities were created. In both cases, AF was induced by a protocol applied in the pulmonary vein area.

The source description used for computing the electric field generated by the 800,000 units was the double layer (EDL). It comprised 1297 elements, evenly distributed over the surface bounding atrial mass. The strength of the elements was proportional to the time course of the membrane potential (TMP) of the nearest unit, specified at 1 ms intervals [7]. The effect of volume conduction inhomogeneities on the atrial contribution to body surface potentials was computed by means of the boundary element method. It involved a multi-compartmental torso model including blood cavities of both the atria and the ventricles, the lungs and the thorax boundary [7]. Body surface potentials were computed at 590 points distributed over the torso surface; the electrode locations of the 12-lead ECG formed a subset.

2.2. Signal processing

The general comments on the global dynamics of the AF variants presented below are based on the visual inspection of animations of the TMP distribution on the atrial surface.

The timing of the upstrokes of the transmembrane potentials assigned to the EDL source elements was taken as the marker of the timing of local depolarization. For each source element, the number of upstrokes observed within a given time interval is referred to as the local firing rate *FR*. The resulting values were mapped on the atrial surface.

For each of the 590 field points on torso surface, the time course of the simulated potentials were documented, using the Wilson Central terminal as the reference. The amplitude spectra of all 590 lead signals were computed by means of the Discrete Fourier Transform; no anti-aliasing filtering was applied. For spectra computed over a period of P seconds the resulting frequency resolution is $1/P$ (Hz). In each of the resulting spectra the dominant frequency *DF* was, in a crude fashion, taken to be the frequency displaying the largest amplitude. The spectra shown are normalized to signal power.

Descriptive statistics are specified by mean $\pm$ SD.

3. Results

The two simulated cases presented differ by the complexity of their dynamics and their atrial firing rate patterns.

Case I

The dynamics of Case I was characterized by 1-to-3 wavelets having wavelengths of 6.2 $\pm$ 2.7 cm. Two stable rotors were present, both having a frequency of about 4 Hz, one of them rotating clockwise (as viewed from outside the heart) around the tricuspid valve, the other, around the superior vena cava.

The distribution of the firing rates over the atrial surface was stable and almost uniform: FR=3.85 $\pm$ 0.11 Hz estimated from an 8-second period.

Similarly, the distribution of the *DF*s over the thorax surface was stable and almost uniform: DF=4.08 $\pm$ 0.24 Hz estimated from the same 8-second period.

An example of the accompanying wave forms is presented in Fig. 1. It shows (upper trace) the TMP at the source element closest to the sensing electrode of lead V1 and (lower trace) the corresponding, simulated ECG of lead V1.

The amplitude spectrum of the V1 signal estimated from the same 8-second period is shown in Fig. 2.

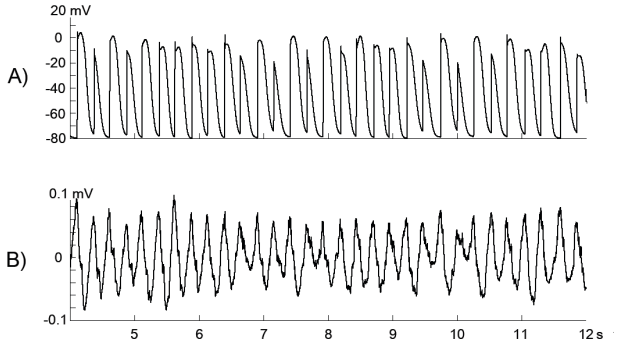

Figure 1. Case I. Panel A: TMP acting as the strength of the EDL source element closest to electrode V1, shown over a time interval period of 8 s. Panel B: Corresponding V1 signal.

Case II

In contrast to Case I, the dynamics observed in the non-uniform substrate of Case II was far less stable. Up to six wavelets were found. Moreover, different transitions in the dynamics were observed, occurring at irregular intervals. Here we describe one such transition.

As in Fig. 1, Fig. 2 depicts (upper trace) the TMP at the source element closest to the sensing electrode of lead V1 and (lower trace) the corresponding, simulated ECG of lead V1, now for Case II. Between t=19 and t=20 a visual inspection of panel B reveals a clear transition. The dynamics preceding the transition included a stable rotor

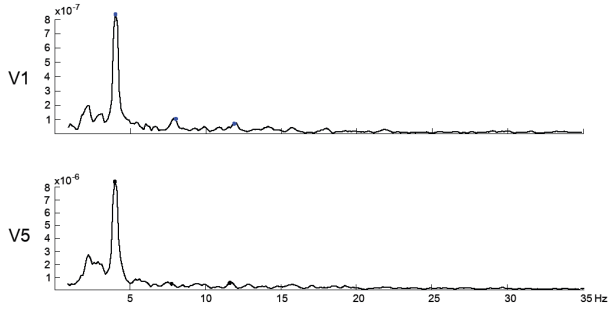

Figure 2. Case I. Panel A: Amplitude spectrum of the signal of lead V1 shown in Fig. 1B. Panel B: corresponding spectrum of lead V5.

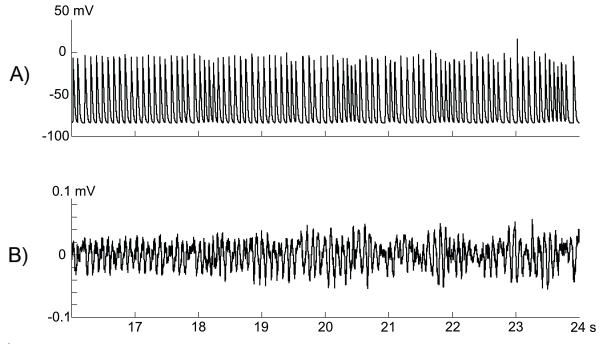

Figure 3. Case II. Panel A: TMP acting as the strength of the EDL source element closest to electrode V1, shown over a time interval period of 8 s. Panel B: Corresponding V1 signal.

at a frequency of 14 Hz, rotating clockwise around the left atrial appendage. A second one was found, rotating at a frequency of about 11 Hz around the lower right pulmonary vein. The latter triggered a wide wave front on the right atrial surface, propagating from left to right.

During the period following the transition, a stable rotor was present, rotating clockwise around the left atrial appendix at 14 Hz, a stable rotor rotating the lower right pulmonary vein at about 11 Hz, accompanied by unstable re-entries set up over the frontal part of the right atrium.

The amplitude spectra of leads V1 and V5 during 8-second intervals preceding and following the transition are shown in Fig. 4 and Fig. 5, respectively .

Although only slight shifts following the transition were observed in the distribution of *FR* over the atrial surface, the transition was clearly noticeable in the distributions of the DF on the torso surface. This is illustrated in Fig. 6.

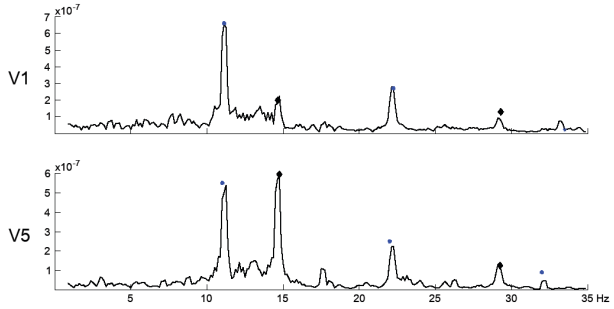

Figure 4. Case II. Amplitude spectra of the ECG of lead V1 (upper trace) and V5 (lower trace) computer over the interval *preceding* the transition. The observed basic frequencies and their higher harmonics in the frequency range shown are marked.

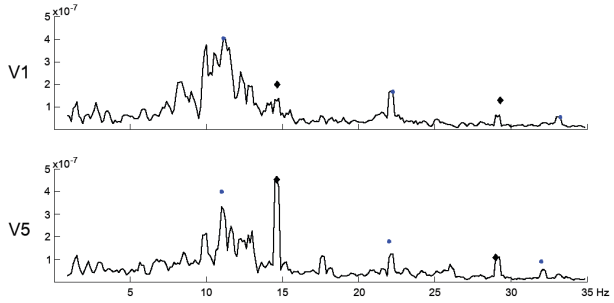

Figure 5. Case II. Amplitude spectra of the ECG of lead V1 (upper trace) and V5 (lower trace) computer over the interval *following* the transition. The observed basic frequencies and some of their higher harmonics harmonics are marked.

4. Discussion and conclusions

Simulation studies such as the one discussed here permit the study of AF related signals under fully controlled conditions and in complete absence of interference of signal component generated by ventricular activity. The two cases presented here span a wide range of possible mechanisms of AF, and permit the study of their expression on body surface potentials.

The global description of the dynamics of Case I suggests a flutter-like phenomenon. The accompanying distribution of the FR is almost uniform. The stability of the FR as well as that of the DF seems to confirm this. However, the spurious wavelets set up at around the regions of the colliding wave fronts of the two rotors complicate matters. In the amplitude spectrum their effect is represented by the wide elevation of the spectrum to the left of the peak of the DF.

Case II is clearly the more interesting one. The two rotors have different frequencies, both higher than in Case I.

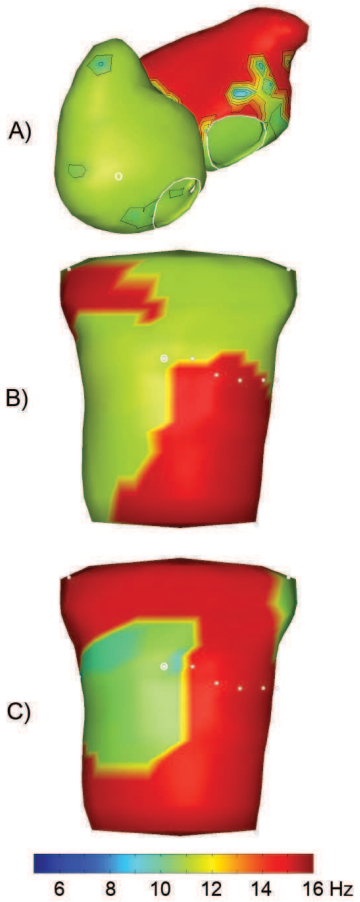

Figure 6. Case II. Panel A. Distribution of the firing rate *FR* preceding the transition mapped on the atrial surface. Panel B: Distribution of the DF computed from the period preceding the transition mapped on the torso surface. Panel C: distribution of *FR* following the transition. All geometries shown in the natural, frontal view.

Prior to the transition, two distinct basic frequencies were observed (Fig. 4), each corresponding to those of the two major rotors. Classifying this spectrum by its DF (only) would clearly obscure the view on the complexity of the underlying phenomena. The identification of both spectral peaks is facilitated by considering the presence of their harmonics. This holds true even more so if the dynamics is more complex, as was the case after the transition (compare Fig. 4 and Fig. 5). A correct interpretation is also hampered if the time interval on which the spectrum is based is taken too tightly, or if inappropriate anti-aliasing filters are employed. The latter is frequently the case in applications of standard power spectrum tools provided in software packages.

The results indicate that the full Fourier spectrum yields more information about the complexity of a particular variant of AF than the analysis of merely its dominant frequency. The same holds true for analyzing the spectra of multiple lead signals rather using observations from a single lead.

Acknowledgements

This study was made possible by grants from the Swiss National Science Foundation, the Theo-Rossi-Di-Montelera Foundation and the Swiss Governmental Commission of Innovation Technologies.

References

[1] Stanton MS, Miles WM, Zipes DP. Atrial Fibrillation and Flutter. W.B. Saunders Compagny, 1990.

[2] Ropella K, Baerman J, Swiryn S. Effects of procainamide on intra-atrial electrograms during atrial fibrillation: implications for detection algorithms. Circulation 1988;77:1047–1054.

[3] Lazar S, Dixit S, Marchlinski FE, Callans DJ, Gerstenfeld EP. Presence of left-to-right atrial frequency gradient in paroxysmal but not persistent atrial fibrillation in humans. Circulation 2004;110:3181–3186.

[4] Bollmann A, Husser D, Mainardi L, Lombardi F, Langley P, Murray A, J RJ, Millet J, Olsson SB, Stridth M, Sörnmo L. Analysis of surface electrocardiograms in atrial fibrillation: techniques, research, and clinical applications. Europace 2006;8(11):911–926.

[5] Lemay M, Vesin JM, van Oosterom A, Jacquemet V, Kappenberger L. Cancellation of Ventricular Activity in the ECG: Evaluation of novel and existing methods. IEEE Trans Biomed Eng 2007;BME-53/3:542–546.

[6] Ng J, Kadish A, Goldberger J. Effect of electrogram characteristics on the relationship of dominant frequency to atrial activation rate in atrial fibrillation. Heart Rhythm 2006; 3(11):1295–1305.

[7] van Oosterom A, Jacquemet V. Genesis of the P wave: atrial signals as generated by the equivalent double layer source model. Europace 2005;7(suppl. 2):S21–S29.

[8] Courtemanche M, Ramirez RJ, Nattel S. Ionic mechanisms underlying human atrial action potential properties: Insights from a mathematical model. Am J Physiol 1998;275:H301–H321.

[9] Jacquemet V, Virag N, Kappenberger. Wavelength and vulnerability to atrial fibrillation: Insights from a computer model of human atria. Europace 2005;7(suppl. 2):S83–S92.

Address for correspondence:

Mathieu Lemay
EPFL – STI – ITS – LTS1, Station 11
CH-1015 Lausanne, Switzerland
mathieu.lemay@epfl.ch